



# **MIC 2015**

**2015 2nd International Conference on Modelling,  
Identification and Control**

**August 9-10, 2015, Paris, France**



**ATLANTIS  
PRESS**

# *Proceedings*

---

## **2015 2nd International Conference on Modelling, Identification and Control (MIC 2015)**

August 9-10, 2015, Paris, France

# **MIC 2015**



**ATLANTIS  
PRESS**

[www.atlantis-press.com](http://www.atlantis-press.com)  
8 Square des Bouleaux,  
75019 Paris, France

Design and Realization of Improved Image Restoration Method Based on Fuzzy Projection onto Convex Sets <i>Xin Li</i> .....	64
Adaptive Control of Vehicle Position with Non-linearizable Feedback <i>Viacheslav Pshikhopov, Mikhail Medvedev, Victor Krukhmalev</i> .....	68
The Design of Greenhouse Environment Control System Based on LabVIEW, ZigBee <i>Lei Wang</i> .....	74
Design and Implementation of Multimedia Material Library Based on Campus Network <i>Chenyang Yang</i> .....	78
Research Method of Forecasting the Equipment Maintenance and Ordnance Demand <i>Xiuhua Wang, Zhengping Shu</i> .....	81
Regional Industrial Water Demand Prediction Based on Improved Series Gray Neural Network <i>Zhen-Yun Hu, Zhi-Ming Chen, Wei Zhang</i> .....	85
A Full-wave Rectifier Based on Memristive Systems <i>Jiri Vavra, Dalibor Biolek</i> .....	91
FEM Analysis of the Different Spinning Speeds of Inner Groove Copper Tube Formed <i>Shigang Wang, Boyu Zhao</i> .....	95
Performance Analysis on Taper Roller Bearing System Based on Romax <i>Yuanji Wan, Shigang Wang, Le Gu, Fengjuan Wang</i> .....	100
Research on Feature Extraction Curves and Surfaces in Reverse Engineering <i>Linzhe Ao, Shigang Wang, Shufeng Jiang, Shengyuan Jiang</i> .....	104
Surface Reconstruction Based on Reverse Engineering and Testing <i>Shigang Wang, Yong Yan, Shufeng Jiang, Fengjuan Wang</i> .....	109
Thinking Method of Product Form Design of Bionics Based on Nine Screens <i>Shigang Wang, Jie Zhang, Xifeng Wang, Fengjuan Wang</i> .....	113
Weight Analysis of QoS Based Cloud Evaluation Index System <i>Cong Cheng</i> .....	118
Supply Chain Logistics Business Process Reengineering of Automobile Spare Parts Based on SCOR <i>Ming Li, Fangli Qin, Xiang Zhai</i> .....	122

Development of Portable Bridge Strain Detector <i>Nan Zhang, Jiangang Qiao</i> .....	127
Data Preprocessing and Classification for Taproot Site Data Sets of PANAX NOTOGINSENG <i>Dao Huang, Jin He</i> .....	131
Qualitative Research on Frequency -Frequency Rank Distribution of Ancient Chinese Characters in Corpus <i>Haoyang Tian, Ying Liu</i> .....	135
An Improved Stereo Matching Algorithm Based on Guided Image Filter <i>Ruidong Gao, Yun Chen, Lina Yan</i> .....	139
A New Fractal Hyperspectral Image Compression Algorithm <i>Yun Chen, Ruidong Gao</i> .....	145
On Generalized Order of Vector Dirichlet Series of Fast Growth <i>Wanchun Lu</i> .....	151
Study of Numerical Method of Synthetical Surface Heat Transfer Coefficient on Rail during Spraying Process <i>Ge Li, Zhimin Liu, Lin Chen</i> .....	155
Musical Signal Processing Based on Digital Signal Processing Technology <i>Yuying Liu, Liangliang Chen</i> .....	159
Research Based on the Frequency Hopping Wireless Communication Networks <i>Shuang Wu, Ke Zhao</i> .....	163
Blocking Temperature and Hysteresis Characteristics of the Decay Products TITANOMAGNETITES <i>Afremov Leonid, Maria Shmykova, Iliushin Ilia</i> .....	167
Hysteresis Characteristics of Interacting Fe/Fe <sub>3</sub> O <sub>4</sub> Core/Shell Nanoparticles <i>Anisimov Sergei, Afremov Leonid, Iliushin Ilia</i> .....	171
High-k Gate Stacks Influence on Characteristics of Nano-scale MOSFET Structures <i>Konstantin O. Petrosyants, Dmitriy A. Popov</i> .....	174
The Density of Gaps in the Seal Joint in Elastic Contact of Microasperities <i>Peter M. Ogar, Denis B. Gorokhov, Artem S. Kozhevnikov</i> .....	177



# High-k Gate Stacks Influence on Characteristics of Nano-scale MOSFET Structures

Konstantin O. Petrosyants  
 Dept. of Electr. Eng., NRU HSE MIEM; Dept of Analog  
 Circ. Des., IDPM RAS, Moscow, Russia  
 kpetrosyants@hse.ru

Dmitriy A. Popov  
 Dept. of Electr. Eng, NRU HSE MIEM, Moscow, Russia  
 dapopov@hse.ru

**Abstract**—The models of electro-physical effects built-into Sentaurus TCAD have been tested. The models providing an adequate modeling of deep submicron high-k MOSFETs have been selected. The gate and drain leakage currents for 45 nm MOSFET with PolySi gate and SiO<sub>2</sub>, SiO<sub>2</sub>/HfO<sub>2</sub> and HfO<sub>2</sub> gate dielectrics have been calculated using TCAD. It has been shown that the replacement of traditional SiO<sub>2</sub> by an equivalent HfO<sub>2</sub> dielectric considerably reduces the gate leakage current by several orders due to elimination of the tunneling effect influence. Besides, the threshold voltage, saturation drain current, mobility, transconductance, etc. degrade within 10-20% range.

**Keywords-component:** MOSFET; high-k materials; TCAD; physical models.

## I. INTRODUCTION

In novel microprocessors produces by Intel, AMD, Apple, Samsung, NEC Electronics high-k gate CMOS devices are used. In recent years high-k gate nano-scale MOSFETs became to real candidates to reduce standby power consumption of CMOS VLSIs due to their possibility in reduction of gate leakage current in comparison with conventional silicon dioxide gate structures. In previous works the electro-physical behavior of unirradiated high-k gate MOSFETs using Sentaurus [1]-[4] and ATLAS [5], [6] device modeling tools was analyzed. However, the use of high-k gate dielectric also effects the rest characteristics of MOSFETs which need to be studied in detail.

In our work according to the modeling and design strategy for nanoelectronics devices supported by European Nanoelectronics Initiative Advisory Council we have realized the TCAD modeling procedure to achieve close match between TCAD modeling results and experimental characteristics.

## II. PHYSICAL TCAD MODELS

All the physical models of mobility, scattering, carrier transport, tunneling, quantization, generation-recombination, hot-carrier injection implemented in Sentaurus version J-2014.09 were examined. The set of adequate models was selected and recommended for high-k gate MOSFET design (see Table I).

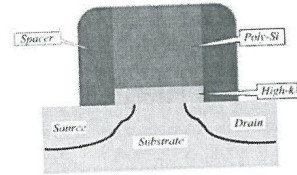


Figure 1. MOSFET structure with high-k gate insulator.

TABLE I. SET OF TCAD PHYSICAL MODELS FOR HIGH-K SIMULATION

Models	Gate Oxide	
	SiO <sub>2</sub>	SiO <sub>2</sub> /HfO <sub>2</sub> / HfO <sub>2</sub>
Transport Model	Hydrodynamic	
Carrier-Carrier Scattering	CarrierCarrierScattering(BrooksHerring)	
Mobility Degradation	Enormal	Enormal (Lombardi, highk)
—Generation—Recombination	SRH(DopingDep), Auger	
Quantization	Density Gradient Quantization Model	
Tunneling	DirectTunneling	
Hot-Carrier Injection	Lucky	

The experimental works [7]-[16] where the main physical parameters describing the silicon-dioxide surface discrete trapped charges; device doping profiles; electron and hole mobilities of conventional and SOI FETs with different gate stack and others were analyzed. The real input data for the physical parameters used in Sentaurus tool for different high-k gate FET structures simulation were established.

In [6]-[8] have shown that the carriers capture more intense at HfO<sub>2</sub>/Si interface than at SiO<sub>2</sub>/Si interface. The values of the surface states charge (Q<sub>int</sub>) for SiO<sub>2</sub>, HfO<sub>2</sub> and SiO<sub>2</sub>/HfO<sub>2</sub> dielectrics assumed to be 5·10<sup>10</sup>, 5·10<sup>11</sup> and 1·10<sup>12</sup> cm<sup>-2</sup> respectively. Similar Q<sub>int</sub> values are used in [5] and [6].

Direct Tunneling model parameters were modified with using [9].

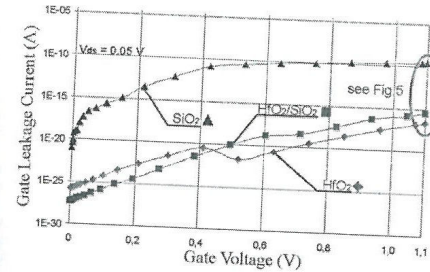


Figure 2. Gate leakage current for high-k MOSFETs with different gate oxide.

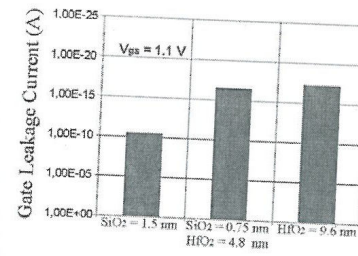


Figure 3. Comparison of Gate leakage current for high-k MOSFETs with different gate oxide.

## III. 45NM MOSFET MODELING

The calibration of electrical characteristics for different high-k gate MOSFETs was carried out comparing I-V characteristics obtained from TCAD simulations and those from measurements.

45nm MOSFET structure with polysilicon gate (W<sub>poly</sub> = 500 nm, L<sub>poly</sub> = 45nm) was simulated. Different gate dielectric: SiO<sub>2</sub>, HfO<sub>2</sub> and composite (stack) of SiO<sub>2</sub> and HfO<sub>2</sub> were used. For all modeled MOSFET structures EOT was set at 1.5 nm (see. Fig.1).

$$EOT = t_{high-k} \cdot \left( \frac{k_{SiO_2}}{k_{high-k}} \right)$$

The doping of the silicon source/drain region is assumed to be 1·10<sup>20</sup> cm<sup>-3</sup>. The peak value of doping concentration in silicon channel region is assumed to be 1·10<sup>18</sup> cm<sup>-3</sup>.

The doping concentration in polysilicon gate is 1·10<sup>22</sup> cm<sup>-3</sup> at the top and 1·10<sup>20</sup> cm<sup>-3</sup> at bottom of the polysilicon gate.

Threshold voltage (V<sub>th</sub>), drain leakage current (I<sub>off</sub>) and gate leakage current (I<sub>gate</sub>) were calculated at a lower voltage (V<sub>ds</sub>=0.1 V, V<sub>gs</sub> from 0 to 1.0 V). Saturation drain current (I<sub>sat</sub>), mobility (μ) and transconductance (S) were calculated at a high voltage (V<sub>ds</sub>=1.0 V, V<sub>gs</sub> from 0 to 1.0 V). The values of the basic parameters for 45nm MOSFET with the three types of gate dielectric are collected in Table II.

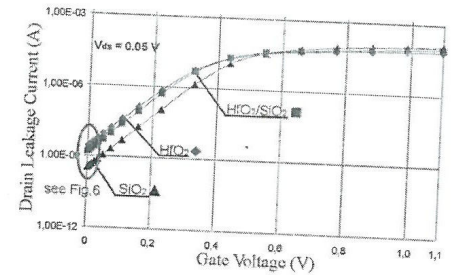


Figure 4. Id-Vg characteristics for high-k MOSFETs with different gate oxide.

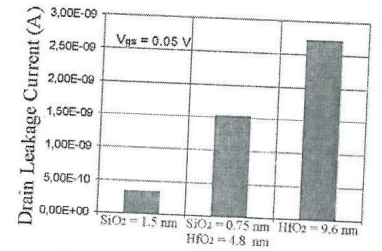


Figure 5. Comparison of Drain leakage current for high-k MOSFETs with different gate oxide.

TABLE II. PARAMETERS OF 45NM HIGH-K MOSFET WITH DIFFERENT GATE OXIDE

Parameters	Gate Oxide		
	SiO <sub>2</sub> 1.5 nm	SiO <sub>2</sub> 0.75 nm / HfO <sub>2</sub> 4.8 nm	HfO <sub>2</sub> 9.6 nm
I <sub>gate</sub> , A	2.82E-10	3.26E-16	2.10E-17
V <sub>th</sub> , V	0.42	0.38	0.37
I <sub>off</sub> , A	3.35E-10	1.53E-09	2.72E-09
I <sub>on</sub> , mA	1.12	1.0	0.84
μ, m/(V·s)	168	133	125
S, uA/V	330	290	210

Table II and Fig. 2 and Fig. 3 show that the gate carrier tunneling effect could be pressed and gate leakage current could be considerably 6-7 orders reduced by replacement traditional SiO<sub>2</sub> gate dielectric of equivalent HfO<sub>2</sub> dielectric.

The rest of important MOSFET parameters: threshold voltage, saturation drain current, mobility, transconductance etc. degrade after replacing SiO<sub>2</sub> with HfO<sub>2</sub> in MOSFETs with polysilicon gate (see Fig.3-Fig.6).

The presented TCAD simulation results agree with experimental I-V characteristics investigations [1], [4] and [13].



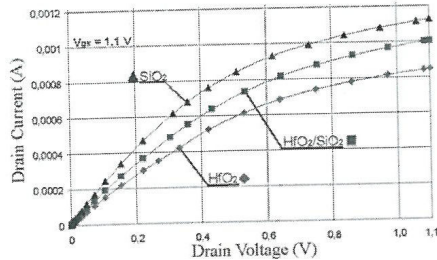


Figure 6. Id-Vd characteristics for high-k MOSFETs with different gate oxide.

#### IV. CONCLUSION

The physical TCAD models providing an adequate modeling of deep submicron high-k MOSFETs have been selected. I-V characteristics of 45 nm high-k gate MOSFET on bulk substrate were simulation with selected models to confirm their adequacy.

#### ACKNOWLEDGMENT

This work was supported by the National Research University–Higher School of Economics Academic Fund Program in 2015, grant No. 15-01-0165, and by Russian Foundation for Basic Research, grant No.14-29-09145.

#### REFERENCES

- [1] A. K. Rana, N. Chand, V. Kapoor, "TCAD Based Analysis of Gate Leakage Current for High-k Gate Stack MOSFET", ACEEE Int. Journ. on Communication, Vol. 2, No.1, Mar. 2011, pp. 5-8.
- [2] S. Chander, P. Singh, S. Baishya, "Optimization of Direct Tunneling Gate Leakage Current in Ultrathin Gate Oxide FET with High-K Dielectrics" IIRDET, No.1, Oct. 2013, pp. 24-30.
- [3] C. Shen, L. T. Yang, G. Samudra, Y. C. Yeo, "A new robust non-local algorithm for band-to-band tunneling simulation and its application to Tunnel-FET", Sol.-St. Electronics Vol. 57, 2011, pp. 23-30.
- [4] S. Yadav, A. Srivastava, J. Rahul, K. K. Jha "TCAD assessment of nonconventional Dual Insulator Double Gate MOSFET", ICDCS, 2012, pp. 462-465.
- [5] N. Shashank, S. Basak, R. K. Nahar, "Design and Simulation of Nano Scale High-K Based MOSFETs with Poly Silicon and Metal Gate Electrodes", International Journal of Advancements in Technology, Vol. 1, No.2, 2010, pp. 252-261.
- [6] N. Shashank, V. Singh, W.R. Taube, R.K. Nahar, "Role of Interface Charges on High-k Based Poly-Si and Metal Gate Nano-Scale MOSFETs", J. Nano- Electron. Phys. 3, No.1, 2011, pp. 937-941
- [7] E. P. Gusev, E. Cartier, D. A. Buchanan, M. Gribelyuk, M. Copel, H. Okorn-Schmidt, C. D. Emic, "Ultrathin high-K metal oxides on silicon: processing, characterization and integration issues", Microelectronic Engineering, 2001, Vol. 59, Iss. 1-4, pp. 341-349.
- [8] W. J. Zhu, T. P. Ma, S. Zafar, T. Tamagawa, "Charge trapping in ultrathin hafnium oxide", IEEE Electron Device Letters, 2002, Vol. 23, Iss. 10, pp. 597-599.
- [9] Y.-C. Yeo, T.-J. King and C. Hu, "MOSFET Gate Leakage Modeling and Selection Guide for Alternative Gate Dielectrics Based on Leakage Considerations", IEEE Transactions on electron devices, Vol. 50, No.4, pp. 1027-1035, April 2003.

- [10] A. Asenov, G. Roy, A. Erlebach, A. Wettstein, S. Motzny, S. Reggiani et al., "Analysis of Dominant Variability Sources in 45nm Planar Bulk CMOS Technologies and Prototype Implementations of the Treatment of Individual Dopants and Traps in Device Modeling Tools", MODERN Consortium, February 2010, pp. 1-48.
- [11] Y. Y. Fan, Q. Xiang, J. An, L. F. Refister, S. K. Banerjee, "Impact of interfacial layer and transition region on gate current performance for high-K gate dielectric stack: its tradeoff with gate capacitance", IEEE Trans Electron Device 2003, Vol. 50, Issue 2, pp. 433-439.
- [12] H.-L. Lu, D. W. Zhang, "Issues in High-k Gate Dielectrics and its Stack Interfaces", High-k Gate Dielectrics for CMOS Technology, Aug 2012, pp. 31-59.
- [13] R. Chaujar, R. Kaur, M. Saxena, M. Gupta, R. S. Gupta, "TCAD assessment of gate electrode workfunction engineered recessed channel (GEWE-RC) MOSFET and its multilayered gate architecture, Part I: Hot-carrier-reliability evaluation", IEEE Transactions on Electron Devices, Vol. 55, No.10, 2008, pp. 2601-2613.
- [14] N.A. Chowdhury, D. Misra, "Charge Trapping at Deep States in Hf-Silicate Based High-k Gate Dielectrics", J. Electrochem. Soc., 2007, Vol. 154, No. 2, pp. G30-G37.
- [15] W. J. Zhu, T. P. Ma, "Temperature Dependence of Channel Mobility in HfO<sub>2</sub>-Gated NMOSFET's", IEEE Electron Device Lett, 2004, Vol. 25, No. 2, pp. 89-91.
- [16] E. Nadimi, G. Roll, S. Kupke, R. Ottking, P. Planitz, C. Radehaus et al., "The Degradation Process of High-k SiO<sub>2</sub>/HfO<sub>2</sub> Gate-Stacks: A Combined Experimental and First Principles Investigation", IEEE Transactions On Electron Devices, Vol. 61, No. 5, May 2014.

## The Density of Gaps in the Seal Joint in Elastic Contact of Microasperities

Peter M. Ogar<sup>a</sup>, Denis B. Gorokhov<sup>b</sup>, Artem S. Kozhevnikov<sup>c</sup>  
Bratsk State University, Bratsk, Russia  
<sup>a</sup>ogar@brstu.ru, <sup>b</sup>denis\_gorokhov@mail.ru, <sup>c</sup>kozhevnikovart@inbox.ru

**Abstract**—Initially, a contact between a rigid rough surface and a homogeneous elastic half-space without taking into account the mutual influence of microasperities is considered. To determine the dependence of the density of gaps in the joint on dimensionless the force elastic geometrical parameter, the discrete roughness model presented by microasperities in the form of equal spherical segments with the height distribution corresponding to the bearing profile curve of the real surface is used. To determine the volume of intercontact space, the volumes of gaps attributable to the single contacting or noncontacting asperities are determined. In this case the equations describing the sections of surfaces of contacting or noncontacting asperities and the half-space under load are used. Then we consider a contact between a rigid rough surface and a layered half-space consisted of the coating with thickness  $\delta l$  and the substrate. By using the stiffness model of a layered half-space, the elastic characteristic are determined for every contacting asperity. The system of transcendental equations which allow to determine the dependence of the density of gaps in case of contact through coating layer on the roughness parameters, material properties, coating thickness and applied load is given. The characteristic curves showing the dependence of the density of gaps in the joint for different coating thickness are given.

**Keywords**— rough surface, spherical asperity, elastic contact of asperities, volume of gaps, density of joint, thin-layer coatings, layered elastic half-space.

#### I. INTRODUCTION

A promising way to increase seals and friction joints' operational factors is the surfacing polymeric covering on their work surfaces anti-frictional films. Operation experiment has shown that the sealing ability anti-friction properties are determined not only by the properties, but also the thickness of the coating material [1]. Long experience of the authors in improving the methods of calculation of tightness of joints show that the density of gaps and in the seal junction and the relative contact area are the critical characteristics. The influence of coating thickness on the relative area for different types of contact is considered in [2, 3]. At the same time, there are no data of the influence of coating thickness on the density of gaps in the joint. It has defined the purpose of the present paper.

#### II. CONTACT BETWEEN A ROUGH SURFACE AND A HOMOGENEOUS ELASTIC HALF-SPACE

We use the discrete model of a rough surface, in which microasperities are presented by identical spherical segments with the distribution of segments' peaks on height corresponds to the bearing profile curve of the real surface

[4]. To describe the distribution of the reference curve is used incomplete beta function:

$$\eta(\varepsilon) = \frac{B_\varepsilon(\alpha, \beta)}{B(\alpha, \beta)} \quad (1)$$

Where  $B_\varepsilon(\alpha, \beta)$  and  $B(\alpha, \beta)$  are incomplete and complete beta functions;

$$\alpha = \left( \frac{R_p}{R_q} \right)^2 \left( \frac{R_{\max} - R_p}{R_{\max}} \right) - \frac{R_p}{R_{\max}}, \quad \beta = \alpha \left( \frac{R_{\max}}{R_p} - 1 \right); \quad (2)$$

Where  $R_p$ ,  $R_q$ ,  $R_{\max}$  are height roughness parameters according to ISO 4281/1-1997.

In this case, the density of the asperities distribution on height function is

$$\varphi'_n(u) = \frac{u^{\alpha-2}(1-u)^{\beta-2}[(\alpha-1)(1-u) - (\beta-1)u]}{\varepsilon_s^{\alpha-1}(1-\varepsilon_s)^{\beta-1}}, \quad (3)$$

Where  $\varepsilon_s$  is determined from the condition  $\varphi_n(\varepsilon_s) = 1$ ,  $\omega R_{\max}$  is the height of a spherical segment,  $\omega = 1 - \varepsilon_s$ .

The radius of the spherical segment is

$$r = \frac{a_c^2}{2\omega R_{\max}}, \quad (4)$$

Where  $a_c$  is the radius of the base of the spherical segment.

The problem of the density of gaps upon contact between a rigid rough surface and a half-space was considered in [5]. As it follows from [5], to find the volume of intercontact space it is necessary to determine the volume of gaps attributable to the single contacting or noncontacting asperities as

$$V_c = \begin{cases} V_{ri} = 2\pi \int_0^{a_i} [z_{10}(\rho) - z_{20}(\rho)] \rho d\rho, \\ V_{oi} = 2\pi \int_0^{a_{oi}} [z_{1r}(\rho) - z_{2r}(\rho)] \rho d\rho, \end{cases} \quad (5)$$



**ATLANTIS  
PRESS**

*www.atlantis-press.com*  
8 Square des Bouleaux,  
75019 Paris, France



9 789462 520998

ISBN: 978-94-62520-99-8  
Advances in Intelligent Systems Research,  
ISSN:1951-6851, Volume 119